High power pulse amplification of ytterbium-doped double-clad fiber amplifier

Liping Chang (常丽萍), Wei Fan (范 薇), Jialin Chen (陈嘉琳),
Li Wang (王 利), Bai Chen (陈 柏), and Zunqi Lin (林尊琪)

Shanghai Institute of Optics and Fine Mechanics, Chinese Academy of Sciences, Shanghai 201800

Received June 13, 2007

By solving a set of time-dependent equations, the characteristics of the ytterbium-doped double-clad fiber amplifier are presented. Besides the steady state in the fiber of the upper-state population, pump power and amplified spontaneous emission without the input signal, the dynamic characteristics of the high power Gaussian pulse amplification like the evolution of pulse waveform distortion, upper-state population distribution and stored energy and pulse energy of the amplifier under the forward and backward pump, are simulated. The relations between the output pulse energy of the amplifier and the different input pulse peak power or pump power are also discussed. The models and results can provide important guide for the design and optimization of the high power pulse amplification.

OCIS codes: 060.2320, 060.2430.

Ytterbium-doped fiber amplifiers have attracted large interests in many applications, such as power amplification at special wavelength, small-signal amplifiers in fiber sensing applications, chirped-pulse amplification, telecommunications, and medicine, because of its broad gain bandwidth ($\sim$ 975 to $\sim$ 1200 nm), high output power, and excellent power conversion efficiency (up to 80%)[1,2]. A few theoretical models for the double-clad fiber amplifiers have been proposed[3,4]. A set of approximate analytical expressions has been deduced to describe the signals, amplified spontaneous emission, and Rayleigh scattering[5−7]. The pulse amplification is much different from the continuous wave (CW) amplifiers. It is more complicated and usually requires the consideration of the pulse shape evolution, the deviation of the upper-state population distribution, the pulse energy and stored energy of the amplifier because of the time-dependent input pulse signal. Wang *et al.* extendedly analyzed the dynamic characteristics of high power pulse amplification of the double-clad fiber amplifiers in detail, including the Raman effect and heat dissipation in the kilowatt fiber amplifiers, which supplied important theoretical guide for the optimization of the amplifier system[8−10].

In this paper, based on propagation equations, by using the finite-difference method, the high power pulse amplification behavior of the Yb-doped double-clad (YDDC) fiber amplifier under forward and backward pumping is described. Unlike the small-signal input pulse, in the high power amplification system, the pulse shape is seriously deformed. The upper state population distribution is time-dependent on the signal power, and the evolution of pulse energy and stored energy of the amplifier is also presented. The relations between the output pulse energy and input signal peak power or pump power are discussed. The results are important for the design and development of the high power pulse fiber amplification system.

The configuration of the YDDC fiber amplifier is schematically shown in Fig. 1. The fiber with the length of L is angle-cleaved to suppress the reflection and avoid the self-oscillation. Since the amplified spontaneous emission (ASE) plays an important role in an amplifier, it should be taken into account. And the spectrum of the ASE fluctuates greatly with the wavelength in a large regime, so the ASE spectrum is divided into K channels with central wavelengths of λ_k, $k = 1, \cdots, K$, and an even spacing of $\Delta\lambda$. The input pulse is a narrow bandwidth signal with $\Delta\lambda_{\rm s}$ of 2 nm, the spacing time $\Delta\lambda = \Delta\lambda_{\rm s}$ is reasonable. The typical rate equations for YDDC fiber amplifiers[8] are

$$\frac{{\rm d}N_2(z,t)}{{\rm d}t} = \frac{\Gamma_{\rm p}\lambda_{\rm p}}{hcA}[\sigma_{\rm a}(\lambda_{\rm p})N_1(z,t) - \sigma_{\rm e}(\lambda_{\rm p})N_2(z,t)]P_{\rm p}(z,t) - \frac{N_2(z,t)}{\tau} + \sum_k \frac{\Gamma\lambda_k}{hcA}[\sigma_{\rm a}(\lambda_k)N_1(z,t) - \sigma_{\rm e}(\lambda_k)N_2(z,t)] \times[P^+(z,t,\lambda_k) + P^-(z,t,\lambda_k)], \quad (1)$$

$$N = N_1(z,t) + N_2(z,t), \quad (2)$$

$$\pm\frac{\partial P_{\rm p}^{\pm}(z,t)}{\partial z} + \frac{1}{\upsilon_{\rm p}}\frac{\partial P_{\rm p}^{\pm}(z,t)}{\partial t} = -\Gamma_{\rm p}[\sigma_{\rm a}(\lambda_{\rm p})N_1(z,t) - \sigma_{\rm e}(\lambda_{\rm p})N_2(z,t)]P_{\rm p}^{\pm}(z,t) - \alpha(\lambda_{\rm p})P_{\rm p}^{\pm}(z,t), \quad (3)$$

$$\pm\frac{\partial P^{\pm}(z,t,\lambda_k)}{\partial z} + \frac{1}{\upsilon}\frac{\partial P^{\pm}(z,t,\lambda_k)}{\partial t} = \Gamma[\sigma_{\rm e}(\lambda_k)N_2(z,t) - \sigma_{\rm a}(\lambda_k)N_1(z,t)]P_k^{\pm}(z,t,\lambda_k) - \alpha(\lambda_k)P_k^{\pm}(z,t,\lambda_k) + 2\sigma_{\rm e}(\lambda_k)N_2(z,t)\frac{hc^2}{\lambda_k^3}\Delta\lambda + S\alpha_{\rm RS}(\lambda_k)\times P^{\mp}(z,t,\lambda_k), \quad (4)$$

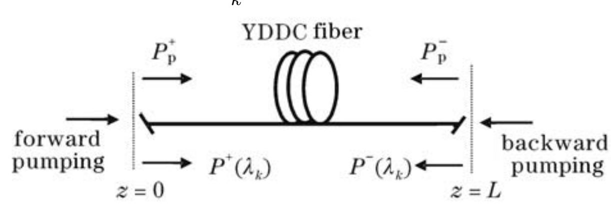

Fig. 1. Configuration of the YDDC fiber amplifier.

1671-7694/2007/110624-04

where c is the light velocity in vacuum. N_1 and N_2, as functions of coordinate z and t, are ground and upper-level populations, respectively. $P_{\mathrm{p}}^{\pm}(z,t)$ is the pump power, and $P^{\pm}(z,t,\lambda_k)$ is the ASE power at the central wavelength of λ_k (positive or negative corresponds to forward or backward propagation, respectively). $P(z,t,\lambda_{\mathrm{s}})$ is the signal power when $k = \mathrm{s}$. This processing is reasonable, because the signal power is much stronger than the ASE power in the corresponding spectral channel ($k = \mathrm{s}$), and the ASE power can be regarded as a weak background noise. The coefficient $\alpha(\lambda)$ represents scattering loss at λ. The parameters Γ_{p} and Γ are the power filling factors for the pump and the ASE (signal), respectively. A is the area of the doped core cross section. α_{RS} is the Rayleigh scattering coefficient, and S is the capture factor of the fiber core. σ_{e} and σ_{a} are the emission and absorption cross sections of ytterbium ions, respectively[1]. τ is the laser upper-level lifetime, and υ_{p} and υ are the group velocity of the pump and ASE (signal), respectively. Here the chromatic dispersion effect is neglected, so υ is independent of the wavelength.

Under forward or backward pumping, the initial boundary conditions associated with the above partial differential equations are

$$P_{\mathrm{p}}^{+}(0) = P_1, \qquad P_{\mathrm{p}}^{-}(L) = P_2, \tag{5}$$

$$P^{+}(0,t,\lambda_k) = 0, \quad P^{-}(L,t,\lambda_k) = 0, \quad k = 1,\cdots,K, \quad k \neq \mathrm{s}, \tag{6}$$

$$P^{+}(0,t,\lambda_{\mathrm{s}}) = P_{\mathrm{s0}}(t), \quad P^{-}(L,t,\lambda_{\mathrm{s}}) = 0, \tag{7}$$

where P_1 and P_2 are the input forward and backward pump powers, respectively. $P_{\mathrm{s0}}(t)$ is the CW or pulse signal power injected into the YDDC fiber amplifier. The stored energy E_{s} in the YDDC fiber, the input pulse energy E_{in} and the pulse energy E_z at the position z of the amplifier are defined as

$$E_{\mathrm{s}}(t) = h\nu_{\mathrm{s}} A \int_0^L N_2(z,t)\mathrm{d}z, \tag{8}$$

$$E_{\mathrm{in}} = \int_{t_1}^{t_2} P^{+}(0,t,\lambda_{\mathrm{s}})\mathrm{d}t, \quad E_z = \int_{(t_1+\frac{z}{\upsilon})}^{(t_2+\frac{z}{\upsilon})} P^{+}(z,t,\lambda_s)\mathrm{d}t, \tag{9}$$

where $h\nu_{\mathrm{s}}$ is the signal photon energy. The stored energy is used to indicate the average upper-level population of the gain medium. t_1 and t_2 are the initial and final values of the duration of the input pulse. This initial-bounary-value problem can be numerically solved through the finite-different method[11].

Prior to the discussion on the pulse amplification, we should assume firstly that the input pulse is coming after the amplifier reaches its steady state without the input signal power. The pump power has a bandwidth of 5 nm and a center wavelength of 915 nm, and the signal wavelength is 1053 nm. Table 1 lists the key parameters used in simulation.

Without the input signal, it can be deduced that $\partial N_2/\partial t = 0$, $\partial P/\partial t = 0$. Figure 2 plots the distribution of upper-level population, pump power and ASE power under the forward pumping or backward pumping power of 10 W.

Table 1. Parameters Used in the Computation

λ_{p}	915 nm	τ	0.90×10^{-3} s
λ_{s}	1053 nm	A	3.4×10^{-11} m^2
λ_1	1019 nm	N	1×10^{26} m^{-3}
λ_K	1101 nm	Γ_{p}	0.0026
$\sigma_{\mathrm{a}}(\lambda_{\mathrm{p}})$	7.92×10^{-25} m^2	Γ	0.56
$\sigma_{\mathrm{e}}(\lambda_{\mathrm{p}})$	2.79×10^{-26} m^2	L	10 m
$\sigma_{\mathrm{a}}(\lambda_{\mathrm{s}})$	9.40×10^{-27} m^2	α	0.003 m^{-1}
$\sigma_{\mathrm{e}}(\lambda_{\mathrm{s}})$	3.77×10^{-25} m^2	$\Delta\lambda$	2 nm

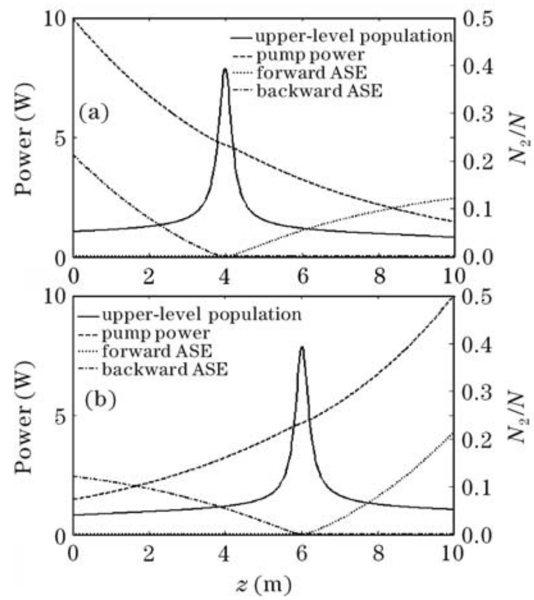

Fig. 2. Steady state distribution of the upper-state population, pump power and ASE power without the input signal, under (a) forward and (b) backward pump power of 10 W.

Under forward and backward pumping, only about 88% of the pump power is absorbed by the YDDC fiber with the length of 10 m. Therefore in the application a longer fiber length should be used so as to make full use of the pump power. Also the upper-state population reaches its maximum of around $z = 4$ m under the forward pumping and $z = 6$ m under the backward pumping, where the total ASE power reaches it minimum, and correspondingly the pump power has a slight deviation. The pump direction only influences the position of the maximum of the upper-state population, but not its distribution curve shape. Based on this steady state of the YDDC fiber amplifier, the dynamic characteristics.

The stored energy and the gain property are determined by the upper-state population of the amplifier to a great extent. Therefore to analyze the time-dependent evolution of the upper-state population is necessary. The input pulse signal is a Gaussian pulse with its full-width at half-maximum (FWHM) of 20 ns. Figures 3 and 4 show the evolution of upper-state population with the small-signal Gaussian (peak power 1 mW) and large-

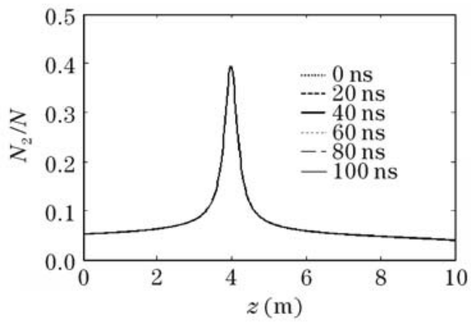

Fig. 3. Evolution of the upper-state population with the small-signal Gaussian input pulse (peak power 1 mW) under 10-W forward pumping.

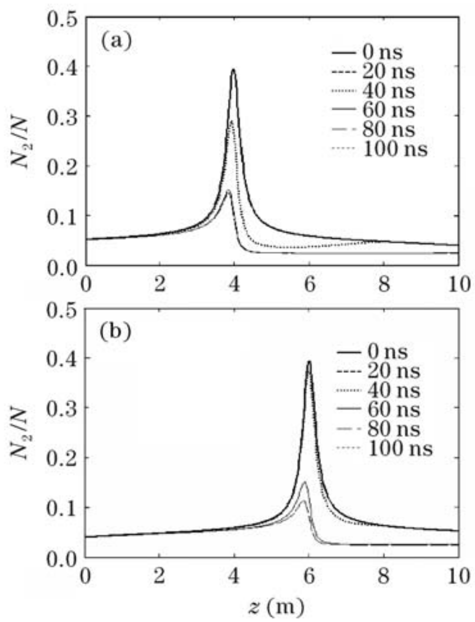

Fig. 4. Evolution of the upper-state population with large-signal Gaussian input pulse (peak power 20 W) under (a) forward and (b) backward pump power of 10 W.

signal Gaussian (peak power 20 W) input pulses under the forward and backward pumping of 10 W.

For the small-signal Gaussian pulse amplification, the distribution of the upper-state population N_2 preserves the same value with time. It also verifies the reason why the pulse shape is not deformed for the small-signal pulse amplification. For the large-signal Gaussian pulse amplification, the strong power consumes the upper-state population gradually with time. We consider the time scale to be $0-100$ ns, between the time $0-20$ ns, the pulse power is relatively low, so the upper-state population is not changed a lot. But when the time turns to be 40 ns, N_2 descends greatly when the pulse power as high enough. Then at the time of 60, 80, and 100 ns, the amplifier has been to the saturated stage and N_2 was preserved low enough. And it should be noted that at the time of 40 ns, the upper distribution N_2 descends more greatly under the forward pumping than the backward pumping, which is due to the pulse power develops more quickly under the forward pumping and consumes a great portion of the upper-state N_2 population.

The evolutions of the pulse energy along the fiber, as well as the stored energy along the time of the amplifier

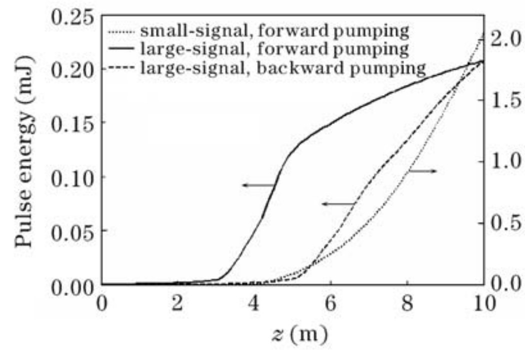

Fig. 5. Pulse energy along the fiber length under the forward and backward pump power of 10 W.

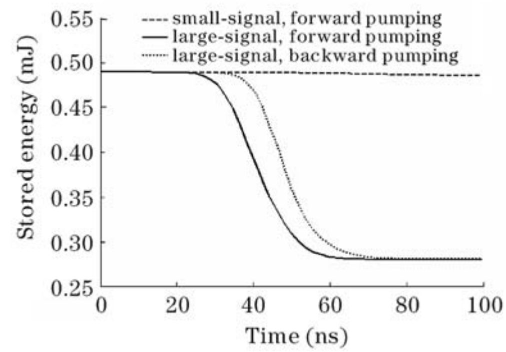

Fig. 6. Evolution of the stored energy under the forward and backward pump power of 10 W.

pumped by 10 W, are depicted in Figs. 5 and 6. For the small-signal amplification under forward pumping, the pulse energy is almost increased exponentially along the fiber. However, for the large-signal pulse it has a great increase at around $z = 3$ m under the forward pumping and $z = 6$ m under the backward pumping where the upper-level population N_2 reaches its maximum at the steady state. Although the final output pulse energy under both forward and backward pumping is almost the same, the evolution process is significantly different because of the different upper-level populations under different pump schemes. At the same time in Fig. 6 the evolution of the stored energy along time of the amplifier shows different characteristics. The stored energy of the small-signal pulse amplification maintains almost the same value, while under forward pumping it begins to descend ahead of that under backward pumping.

As we all know, the output signal resembles the input Gaussian pulse, whereas its leading edge is slightly steepened and trailing is elongated. While to the super-Gaussian pulse, the significant deformation with an extremely high peak power occurs. The pulse width is much narrower than the input pulse. For many applications, such a severe deformation may not be accepted. However, it suggests a method to generate a high peak power and much narrower bandwidth pulse[8]. Figure 7 shows the waveform evolution of the Gaussian input pulse with different input pulse peak power under the forward pumping of 10 W. The time delay for a 10-m-long YDDC fiber is about 49 ns. It can be seen that the distortion of the pulse shape becomes more and more significant as the increasing of input signal peak power. Especially when the input signal peak power reaches

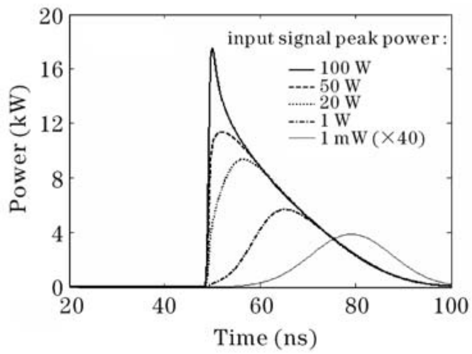

Fig. 7. Waveform evolution of the Gaussian input pulse with different peak powers.

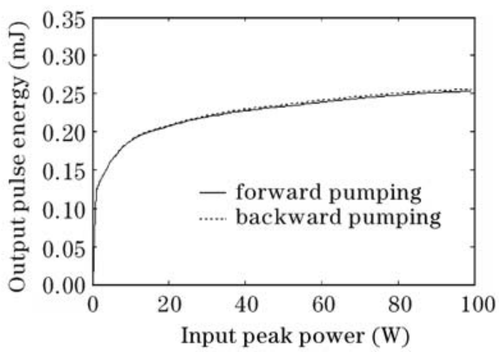

Fig. 8. Output pulse energy versus input peak power under the pump power 10 W.

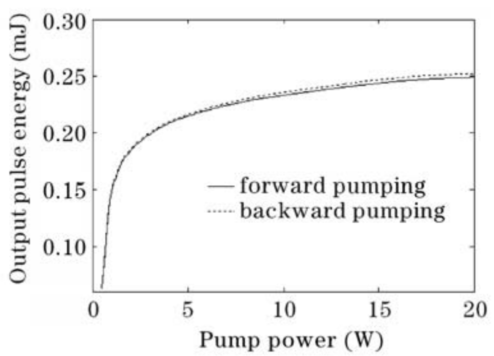

Fig. 9. Output pulse energy versus the pump power with input pulse peak power of 50 W.

100 W, its leading edge is steepened greatly and the peak power up to 17 kW occurs, while the output pulse FWHM becomes narrower at the same time. Therefore it can be seen from Fig. 8 that the pulse energy tends to be saturable when the input pulse peak energy reaches about 40 W, and the output pulse energy has a little difference under both the forward and backward pumping scheme.

The relationship between the output pulse energy and pump power with the input Gaussian pulse peak power of 50 W is depicted in Fig. 9. The output pulse energy under backward pumping is a little higher than that under forward pumping. And the gain of the amplifier is to be the saturation with the pump power up to 6 W, when the upper-state population is almost consumed and the gain is 200 times larger.

By solving a set of time-dependent rate equations associated with the initial boundary conditions, the dynamic characteristics of the high power pulse YDDC fiber amplifier, such as the pulse waveform distortion, the upper state population distribution, pulse energy, stored energy of the amplifier under forward and backward pumping, are presented. The output pulse peak power increases significantly with the increase of the input pulse peak power, but the pulse energy keeps saturable when the input pulse peak energy reaches about 40 W. The evolution of the pulse energy and the stored energy of the amplifier along the fiber length and the time is also analyzed. On the other hand, the relations between the output pulse energy and input signal peak power or the pump power are discussed. These theoretical results are important for the design and optimization of the high power double-clad amplifiers.

L. Chang's e-mail address is changliping@siom.ac.cn.

References

1. R. Paschotta, J. Nilsson, A. C. Tropper, and D. C. Hanna, IEEE J. Quantum Electron. **33,** 1049 (1997).
2. J. Nillson, R. Paschotta, J. E. Caplen, and D. C. Hanna, Opt. Lett. **22,** 1092 (1997).
3. J. Huang, X. Lü, F. Li, C. Gu, A. Wang, H. Ming, Z. Sui, and J. Wang, Chin. J. Lasers (in Chinese) **32,** 1022 (2005).
4. C. Ye, P. Yan, M. Gong, and M. Lei, Chin. Opt. Lett. **3,** 249 (2005).
5. R. Oron and A. A. Hardy, J. Opt. Soc. Am. B **16,** 695 (1999).
6. A. Hardy and R. Oron, IEEE J. Quantum Electron. **33,** 307 (1997).
7. A. A. Hardy and R. Oron, J. Lightwave Technol. **16,** 1865 (1998).
8. Y. Wang and H. Po, J. Lightwave Technol. **21,** 2262 (2003).
9. Y. Wang, J. Lightwave Technol. **23,** 2139 (2005).
10. Y. Wang, IEEE J. Quantum Electron. **40,** 731 (2004).
11. J. Lu and Z. Guan, *Numerical Methods for Partial Differential Equations* (in Chinese) (Tsinghua University Press, Beijing, 1987).